

A data-driven particle filter for lithium-ion batteries state-of-life prognosis

Francesco Cadini¹, Claudio Sbarufatti¹, Francesco Cancelliere², Marco Giglio¹

¹ *Politecnico di Milano, Dipartimento di Meccanica, via La Masa 1, I-20156 Milano, Italy*

*francesco.cadini@polimi.it
claudio.sbarufatti@polimi.it
marco.giglio@polimi.it*

² *Politecnico di Milano, Dipartimento di Energia, via La Masa 34, I-20156 Milano, Italy*

francesco1.cancelliere@mail.polimi.it

ABSTRACT

In recent years, Lithium-Ion rechargeable batteries have quickly become the most popular portable power sources, with applications ranging from consumer electronics (smartphones, laptops, etc.) to electric vehicles and unmanned aerial/space vehicles. Indeed, Li-ion batteries are subject to degradation over time, in particular due to the irreversibility of the electro-chemical processes driving their functioning. The deterioration of the performances is further worsened by the operational and environmental boundary conditions in which they operate (e.g. discharge rates, usage and storage temperatures, etc.). The consequences of unexpected failures due to degradation may range from mild, for example in consumer electronics, to very severe, if not catastrophic, in particular in aerospace applications, both from the economical and the safety points of view. In this context, the prediction of future degradation performances of the batteries plays a fundamental role. In this work, we exploit a recently introduced prognostic algorithmic scheme, which combines the real-time prediction capabilities of particle filters with the flexibility and simplicity of feed-forward neural networks, for adaptively predicting the State-of-Life (SOL), i.e. the capacity, of Li-Ion batteries, on the basis of past and current capacity observations. The major advantage of the proposed method lies in the fact that the algorithm automatically adapts to different degradation dynamics, without the need to derive and/or calibrate any physics-based model. The method is demonstrated with reference to actual Li-Ion battery discharge data taken both from the prognostics data repository of the NASA Ames Research Center database and from literature.

Francesco Cadini et al. This is an open-access article distributed under the terms of the Creative Commons Attribution 3.0 United States License, which permits unrestricted use, distribution, and reproduction in any medium, provided the original author and source are credited.

1. INTRODUCTION

In recent years, Lithium-ion (Li-ion) batteries have gained large popularity as portable energy sources due to their significant advantages with respect to other battery types, such as (K.Goebel, B. Saha, 2008), (Sbarufatti, Corbetta, Giglio, & Cadini, 2017): i) the lower weight, due to the lightweight lithium and carbon-made electrodes, and, at the same time, the larger energy density, due to the high chemical reactivity of lithium; ii) the possibility of being recharged also if they are not completely discharged without any detrimental effects (no memory effect); iii) the lower self-discharge rate, so that they better maintain their charge when not used; iv) the longer life cycle, since they can operate successfully even after hundreds of charge-discharge cycles.

However, due to their rechargeable nature, Li-Ion batteries are subject to irreversible processes occurring during their charging and discharging cycles, such as, for example, the formation of a solid-electrolyte interphase (SEI) (Pinson & Bazant, 2012), which severely affect the batteries' electrochemistry. These processes involve, in general, to a continuous capacity fade, which eventually lead to the battery failure, with consequences ranging from a quite safe need to replace the battery of a mobile phone, to the catastrophic failure of an interplanetary probe (K.Goebel, B. Saha, 2008), (He, Williard, Osterman, & Pecht, 2011).

In order to overcome these issues, many efforts have been devoted in literature to devising proper methods for improving the reliability and the availability of Li-Ion batteries. More specifically, a major role is played by the so-called prognostic and health management (PHM) methods, which, on the basis of different kinds of available, but indirect, information, allow to automatically, and in real-time, track some hidden indicators of the degradation state of the batteries, such as, for example the state-of-health (SOH), the state-of-charge (SOC), the state-of-life (SOL), and at

predicting their remaining useful lifetime (RUL), either in terms of the end-of-discharge (EOD) or the end-of-life (EOL) times, possibly to support condition- or even prediction-based maintenance policies. In this regard, thorough reviews of many advanced PHM methods can be found in (Berecibar, Gandiaga, Villarreal, Omar, Van Mierlo, and Van Den Bossche 2016), (Wu, Fu, & Guan, 2016). Traditionally, these methods are classified in three major families, i.e., model-based, data-driven or hybrid methods, depending on the type and quality of the information used to perform diagnostics and/or prognostics (Guo, Li, & Pecht, 2015). Model-based methods focus on identifying proper relationships between the observable quantities and the indicators of interest by building physics-based models of the degradation processes affecting the battery life. Data-driven methods, on the other hand, aim at mapping the above by some approximating models adaptively built on the basis of available data, such as, for example, neural networks (NN), Gaussian process functional regressions, support vector regressions, fuzzy inference engines, etc. Hybrid methods aim at combining model-based and data-driven methods, when possible, in an attempt to overcome the limitations of the individual methods and, thus, improve diagnostic and prognostic accuracies by better exploiting all the available information. A promising hybrid strategy seems that of resorting to particle filtering-based algorithms, where the required analytical models representing either the dynamic behavior of the system or the measurement equation are actually suitable data-driven surrogate models (Charkhgard & Farrokhi, 2010), (Daroogheh, Baniamerian, Meskin, & Khorasani, 2015). These kind of methods are based on the consideration that, both physics-based model and approximating, surrogate models require the identification of suitable model parameters on the basis of some available observations; however, surrogate models do not require any physics/mathematics-based derivations, which might turn out to be very time consuming, and are generally much computationally faster, especially with respect to numerical models, which might be a critical feature for real-time applications.

One important issue which still severely limits the applicability of these approaches is that the surrogates models are trained off-line on the basis of a set of available examples of the input/output mapping of interest, typically collected under some representative, fixed operative conditions, such some controlled environment in laboratory tests. Actually, this represents a problem also of many other diagnostic/prognostic methods, not restricted to those relying on surrogate modeling. For example, many works of literature demonstrate their proposed methods with reference to Li-ion batteries voltage/capacity laboratory measurements acquired at constant discharge rates/currents. While this approach easily allows to verify the performances of the algorithms and, possibly, to fairly compare them, at the same time it does not account for real operating conditions,

typically requiring varying mission profiles and/or boundary conditions (e.g., temperature, mechanical degradation, lithium metal plating, etc. (Vetter et al., 2005)). Some works of literature have already attempted to address this issue, which requires the capability of quickly adapting to the changing underlying dynamics (Wang, Yang, Zhao, & Tsui, 2017). In (Sbarufatti et al., 2017) some of the same authors of the present work presented a novel hybrid prognostics framework for the prediction of the EOD of Li-ion batteries, where the parameters of the surrogate model, i.e. a radial basis function neural network, were identified on-line by a particle filter on the basis of the real-time observations of the degradation process, thus allowing to naturally capture possible changes of the degradation dynamics and to accordingly update the RUL estimates.

In this context, the first purpose of this work is that of adapting the hybrid approach introduced in (Sbarufatti et al., 2017), which was restricted to the EOD prediction within individual discharge cycles, and inspired by the work in (Doucet et al., 2000), to be able to perform also SOL estimation and predict the EOL of Li-ion batteries. First, we propose to resort to multi layer perceptron (MLP) neural networks, which have turned out to be simpler and more intuitive for this kind of application; then, since, in this case, the algorithm has to predict an individual degradation history, and not several successive discharge curves as in the previous work, a pre-training of the MLP neural network on some reference trajectory is suggested (although not strictly required), so as to significantly restrict the search space of the surrogate model's parameters and speed-up the algorithm convergence. Note that the actual degradation can be significantly different from the pre-training one, as we demonstrate in this work, thus still guaranteeing the adaptation capabilities of the prognostic tool. Moreover, to further increase the algorithm adaptability, the set of particles used by the particle filter (i.e., neural networks weights, see (Sbarufatti et al., 2017)) is artificially enriched by a particle resulting from a back-propagation-based optimization of a network on the basis of the capacity observations available up to the current time.

The proposed method is demonstrated with reference to real degradation transients taken from the NASA Ames Research Center database (Saha & Goebel, 2007) and the CALCE Battery Group (Pecht, 2017). The available trajectories are properly modified in order to be able to test the algorithm in varying operating conditions.

The paper is organized as follow. Section 2 briefly recalls the main features of the method proposed for sequentially train MLP-NN models by means of a particle filter algorithm. The multi layer perceptron-based particle filter (MLP-PF) approach here proposed is then customized in order to perform adaptive prognosis of the EOL of Li-Ion batteries. Section 4 discusses the performances of the proposed method, demonstrating the capability of the algorithm with

reference to the datasets cited above, which are typically used as benchmark case studies in similar works of literature. Section 5 draws some conclusions on the results and proposes future developments of the methodology.

2. MULTILAYER PERCEPTRON PARTICLE FILTER (MLP-PF) FOR SOL PROGNOSIS

This Section first briefly summarizes the method initially proposed by (de Freitas, Niranjan, Gee, & Doucet, 2000) and further investigated and applied to PHM of Li-ion batteries in (Sbarufatti et al., 2017), where NN models were sequentially trained by means of a particle filter algorithm. The multi layer perceptron-based particle filter (MLP-PF) approach here proposed is then customized in order to predict the EOL of Li-Ion batteries and to diagnose their SOH. The interested reader is referred to (Bishop, 1995), and to (Doucet, Godsill, & Andrieu, 2000) and (Arulampalam, Maskell, Gordon, & Clapp, 2007) for thorough descriptions of the functioning of MLPs and particle filters, respectively, and to (de Freitas et al. 2000) for further details on particle filtering-based NN training.

2.1. MLP neural networks basic principles

A schematic view of the MLP network used in this work is shown in Figure 1, where the MLP model aims at approximating the capacity as a function of the number of charge-discharge cycles. The input node represents the number of cycles (k) at which the terminal voltage is measured, whereas the capacity observation (z) is associated to the output node. The output node collects the non-linear outputs from a generic number M of hidden nodes, each one weighted by a factor $\theta_i^{(1,2)}$, and the biases $b_i^{(1,2)}$, $i = 1, \dots, M$. The network parameters are collected in the NN weight vector $\theta \subseteq \Theta \in \mathbb{R}^{n_\theta \times 1}$ and the NN bias vector $\mathbf{b} \subseteq \mathbf{B} \in \mathbb{R}^{n_b \times 1}$. The activation function of the hidden neurons $h(\cdot): \mathbb{R}^{1 \times 1} \rightarrow \mathbb{R}^{1 \times 1}$ is a tan-sigmoid:

$$h(\alpha) = \frac{2}{1 + e^{-2\alpha}} - 1 \quad (1)$$

where α is the generic hidden neuron input, while the output activation function $f(\beta) = \beta$ (with β being the generic node input) is linear. The output of the MLP network in Figure 1 is then calculated as:

$$g(n, \theta, \mathbf{b}) = f \left(\sum_{i=1}^M \left(h \left((k\theta_i^{(1)} + b_i^{(1)})\theta_i^{(2)} \right) + b^{(2)} \right) \right) \quad (2)$$

As a general principle, the number of hidden nodes should be sized according to the complexity of the relationship that has to be learnt by the MLP. Intuitively, the larger the number of hidden neurons, the higher the capability of the algorithm in approximating complex relationships (Bishop, 1995). However, a large number of hidden neurons may give rise to

data over-fitting issues, thus severely hampering the generalization capability of the NN on new data, especially for prediction outside the training domain, which is the case of this work, especially at earlier times. Furthermore, increasing the number of hidden neurons also implies a larger number of unknown parameters network weights) to be identified, which may significantly increase the computational burden of the updating process described later. Similarly to what was done in (Sbarufatti et al., 2017) for the RBF networks, in this application the number of hidden neurons is empirically set to three based on a trial and error procedure. As in (Sbarufatti et al., 2017), according to a qualitative sensitivity analysis performed by the authors, and not shown here for brevity's sake, a slightly larger hidden layer (e.g., 4-7 neurons) still provides satisfactory results.

With this choice of the MLP network structure, we can collect the $n_x = 10$ network parameters in a vector $\mathbf{x} = [x_1, x_2, \dots, x_{10}]^T$, where the elements $x_{1:6}$ are the six connection weights ($\theta_{1:6}$) and the elements $x_{7:10}$ are the four MLP biases ($\mathbf{b}_{1:5}$).

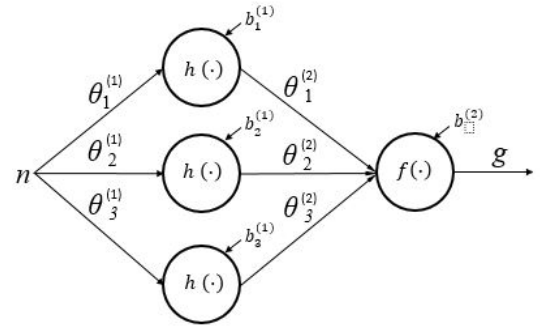


Figure 1: MLP neural network structure.

2.2. MLP-PF for Li-ion batteries EOL prognosis

According to the framework proposed in (Sbarufatti et al., 2017), we introduce a state-space representation of the time evolution of the n_x MLP model parameters (weights and biases), which are collected in the state vector $\mathbf{x} \in \mathbb{R}^{n_x \times 1}$, so that the particle filter aims at sequentially training the MLP. Under the common operative assumption that the process observations are available at discrete cycles, the state space representation then reads:

$$\begin{aligned} \mathbf{x}_k &= \mathbf{x}_{k-1} + \boldsymbol{\omega}_{k-1} \\ z_k &= g(\mathbf{x}_k, k) + \eta_k \end{aligned} \quad (3)$$

where the subscript k is the discrete cycle and, at the same time, the input of the non-linear MLP mapping $g(\cdot)$ in (2), z_k is the output of $g(\cdot)$, i.e., the Li-ion battery capacity, the random process $\boldsymbol{\omega}_k \in \mathbb{R}^{n_x \times 1}$ is the stochastic component of the MLP model parameter evolution and $\eta_k \in \mathbb{R}$ is the measurement noise (Doucet et al., 2000). The evolution of the MLP parameters during their updating process is then modeled as a discrete random walk driven by a process noise

ω_k , large enough to suitably “explore” the parameters’ space and to guarantee a certain degree of flexibility so as to possibly adapt to any, possibly unexpected, changes in the process dynamics.

In this framework, the particle filter is used to recursively estimate the posterior probability density function (pdf) $p(\mathbf{x}_k|\mathbf{z}_{1:k})$ of the MLP parameters \mathbf{x}_k , given the set of observations $\mathbf{z}_{0:k}$ up to the current k -th cycle. As extensively discussed in many works of literature, the nonlinearity of the dynamic state-space model in (3) and/or any non-Gaussianity of the process and/or measurement noises are such that analytical solutions of the optimal prediction-update Bayesian recursion for $p(\mathbf{x}_k|\mathbf{z}_{1:k})$ cannot be obtained (Doucet et al., 2000), (Arulampalam et al., 2007). Thus, the estimation of a sub-optimal solution for the posterior pdf $p(\mathbf{x}_k|\mathbf{z}_{1:k})$ is typically achieved by means of numerical methods, such as direct numerical integration, Gaussian approximations and Monte Carlo (or particle filters) methods. Here, similarly to (Sbarufatti et al., 2017), we resort to the solution based on the sampling importance resampling (SIR) PF algorithm. Then, the Monte Carlo estimator of the MLP weights posterior pdf can be obtained as:

$$\hat{p}(\mathbf{x}_k|\mathbf{z}_{1:k}) \approx \sum_{i=1}^{N_s} w_k^{(i)} \delta(\mathbf{x}_k - \mathbf{x}_k^{(i)}) \quad (4)$$

where the importance samples $\mathbf{x}_k^{(i)}$, $i = 1, \dots, N_s$ are N_s independent and identically distributed realizations of the system state vector, drawn from the importance pdf $p(\mathbf{x}_k|\mathbf{x}_{k-1})$. The terms $w_k^{(i)}$, $i = 1, \dots, N_s$ are the normalized importance weights and $\delta(\cdot)$ is the Kronecker delta.

As proven in (Arulampalam et al., 2007), the normalized importance weights can be recursively computed as:

$$w_k^{(i)} = \frac{\tilde{w}_k^{(i)}}{\sum_{i=1}^{N_s} \tilde{w}_k^{(i)}} \quad (5)$$

where the non-normalized weights $\tilde{w}_k^{(i)}$ are given by

$$\tilde{w}_k^{(i)} = w_{k-1}^{(i)} p(z_k|\mathbf{x}_k^{(i)}) \quad (6)$$

The function $p(z_k|\mathbf{x}_k^{(i)})$ is the likelihood of the observation z_k , i.e., the probability of observing z_k given the underlying non-linear mapping $g(\mathbf{x}_k, t_k)$ is approximated by the i -th MLP model defined by the parameters $\mathbf{x}_k^{(i)}$.

Finally, in order to avoid the sample impoverishment problem (Arulampalam et al., 2007; Doucet et al., 2000), which dramatically reduces the number of samples with non-negligible weights, thus hampering the posterior pdf representation, a resampling scheme is implemented after the weight normalization (Doucet et al., 2000), (Arulampalam et al., 2007).

The estimation of the posterior distribution $p(\mathbf{x}_k|\mathbf{z}_{0:k})$ is carried out each time k a new observation z_k becomes available. The set of samples and associated weights $\{\mathbf{x}_k^{(i)}, w_k^{(i)}\}$ defines a set of N_s MLP network models, which can be used also to predict the future capacity behavior over the charge-discharge cycles and, consequently, the EOL, as it shall be discussed later.

Operatively, we assume that the random walk in (3) is driven by uncorrelated, zero-mean Gaussian noises, i.e., $\omega_k \sim \mathcal{N}(0, \Sigma_{\omega_k})$, where the covariance matrix Σ_{ω_k} is diagonal. In general, the choice of the noise variances is not an easy task: too small values may hamper a proper (and reasonably fast) exploration of the state-space, whereas too large values do not guarantee a satisfactory state estimation, as discussed by many authors in literature. A common approach for achieving a satisfactory trade-off is that of letting the variances decrease from an initial value as the estimation process progresses, so as to guarantee the convergence of the algorithm (Schwunk, Armbruster, Straub, Kehl, & Vetter, 2013), (Gordon, Salmond, & Smith, 1993). In this work, following (Sbarufatti et al., 2017), we propose the following expression for the process noise covariance matrix as a function of the discrete cycle k :

$$\Sigma_{\omega_k} = \left(\sigma_0 e^{-\frac{k}{\sigma_1}} + \sigma_2 \right) \cdot I \quad (7)$$

where the variances of all the parameters \mathbf{x}_k are taken to be the same and I is the $n_x \times n_x$ identity matrix. By using this expression for the variances, we can easily and intuitively set their starting value ($\sigma_0 + \sigma_2$), settling value (σ_2) and rate of decrease ($\frac{1}{\sigma_1}$).

We further assume that the measurement noise η_k is also zero-mean, Gaussian with variance σ_η^2 and independent from k , i.e., $\eta_k \sim \mathcal{N}(0, \sigma_\eta^2)$. According to (Sbarufatti et al., 2017), in order to increase the filter robustness, we choose the particles weights to account for the whole sequence of capacity observations up to the current step k . The likelihood function in (6) then becomes:

$$\begin{aligned} \mathcal{L}_k^{(i)} &= p(z_{1:k}|\mathbf{x}_k^{(i)}) = \\ &= ((2\pi)^{k+1} |\Sigma_\eta|)^{-0.5} \exp \left\{ -\frac{1}{2} \left(z_{1:k} \right. \right. \\ &\quad \left. \left. - g(\mathbf{x}_k^{(i)}, 1:k) \right)^T \Sigma_\eta^{-1} \left(z_{0:k} - g(\mathbf{x}_k^{(i)}, 1:k) \right) \right\} \end{aligned} \quad (8)$$

where the term $z_{0:k}$ represents the sequence of terminal voltage observations in correspondence of the cycle sequence $1:k$ and the terms $g(\mathbf{x}_k^{(i)}, 1:k)$ are the correspondent predictions of the i -th MLP network with parameters $\mathbf{x}_k^{(i)}$.

On the basis of the results obtained in (Sbarufatti et al., 2017), in order to improve the efficiency of the approach, we propose to perform a pre-training of the MLP on the basis of

a properly chosen degradation curve observed in some reference Li-Ion battery. By doing so, in fact, the network weights are expected to reach a region of the parameter space closer to the optimal one for the observations that will be used during the diagnostic/prognostic task. However, Li-Ion batteries may show very different degradation behaviors, due to the operating conditions, the battery types, etc., so that a pre-training on data very different from those that will actually be used might be even misleading. For example, if the pre-training were performed with the CALCE dataset of Figure 2, and then used to perform diagnosis on one of the NASA datasets, then the MLPs outputs would tend to be very small with respect to the current capacity values at earlier times, and would take rather long times to adjust to the new degradation dynamics. In order to overcome this issue and improve the algorithm flexibility and robustness, the observations in the pre-training set are normalized so that i) the first capacity observation (corresponding to $k = 1$) is equal to the first available observation of the new degradation dynamics and ii) the final cycle is 50% larger than the actual one in the training set; the value of this last scale factor, motivated by the fact that, indeed, the final cycle of the new dynamics cannot be a priori known, is chosen on the basis of a trial and error procedure.

Following the approach proposed in (Cadini, Zio, & Avram, 2009), at the current cycle k the posterior pdf of the end of life time (i.e. EOL_k) is then estimated by projecting in the future the predictions of the N_s MLP networks associated to the N_s parameter samples (particles) $\mathbf{x}_k^{(i)}$, $i = 1, \dots, N_s$. Operatively, a set of discrete future charge-discharge cycles $[k + 1, \dots, k + p]$ (with the number of steps ahead, p , properly chosen so as to be sure that each network predicts a failure within this horizon time) is fed to each of the N_s MLP networks; the corresponding outputs, i.e., the capacity predictions at the different cycles, are used to build the sample posterior pdf of the capacity at future cycles. At the same time, the $EOL_k^{(i)}$, $i = 1, \dots, N_s$ predicted by each MLP network are used to build the sample posterior pdf of the EOL_k . The estimates of the posterior pdfs of the future capacities \tilde{z}_{k+l} , $l = 1, 2, \dots$, and of the EOL are operatively obtained as:

$$\begin{aligned} \hat{p}(\tilde{z}_{k+l} | \mathbf{z}_{1:k}) \\ \approx \sum_{i=1}^{N_s} w_k^{(i)} \delta(\tilde{z}_{k+l} - g(\mathbf{x}_k^{(i)}, t_{k+l})) \end{aligned} \quad (9)$$

$$\hat{p}(EOL_k | \mathbf{z}_{1:k}) \approx \sum_{i=1}^{N_s} w_k^{(i)} \delta(EOL_k - EOL_k^{(i)}) \quad (10)$$

Consequently, the remaining useful lifetime of the battery (RUL) at the current cycle k is $RUL_k = (EOL_k - k)$, and its estimated posterior pdf is the same as $\hat{p}(EOL_k | \mathbf{z}_{1:k})$, but shifted by k .

In order to enhance the prognostic capabilities, both in terms of accuracy and stability, improving the strategy suggested in (Sbarufatti et al., 2017), we further modify the algorithm introduced above by empirically enhancing the likelihood function in (8). Operatively, at each cycle k , before the resampling stage, a small number $N_{trivial}$ of particles $\mathbf{x}_k^{(i)}$, $i = 1, \dots, N_{trivial}$ (i.e., the MLP network parameters) are substituted by a new particle (called hereafter “trivial”) built by training the same MLP network architecture with a set made up of the actual sequence of degradation observations $\mathbf{z}_{1:k}$ up to the current cycle k and the observations $\mathbf{z}_{k+1:end}$ of the initial pre-training set, after properly normalizing them according to a procedure similar to that illustrated for the first training of the MLP, so as to smoothly connect the two observation sequences. This scheme is qualitatively shown to significantly improve the prognostic performances with the parameter $N_{trivial}$ ranging between 1 and 10. In fact, a few particles with a good behavior up to (at least) the current cycle k should contribute to maintain the whole particle swarm “close” to the actual degradation dynamics, especially when unexpected behaviors of the observations and/or exceedingly deviated values of the noises occur. On the other hand, using a too large number of identical “trivial” particles would tend to be equivalent to directly using the trivial MLP for the predictions, thus not exploiting the filtering capabilities of the filter.

3. RESULTS

In this Section we demonstrate the prognostic capabilities of the proposed algorithm, with reference to the SOL datasets by the Prognostic Center of Excellence at NASA Ames Research Center (Saha & Goebel, 2007) and of the CALCE Battery Group (Pecht, 2017), shown in Figure 2. In particular, the datasets labeled “NASA 1, 2 and 3” are taken from the NASA Ames research center database, whereas the one labeled “CALCE” is taken from the CALCE database. Note that these datasets are obtained under controlled laboratory conditions and at constant discharge rates (constant current).

According to the initialization procedure illustrated in Section 2, for convenience, but with no loss of generality, NASA 2 is chosen as the pre-training dataset for the MLP networks, as it shows the broader range of variation of its capacity. The PF-MLP algorithm is run with $N_s = 500$ particles; a larger number of particles would excessively slow down the algorithm, with no benefits in terms of mean of the RUL posterior pdf $\hat{p}(EOL_k | \mathbf{z}_{1:k})$, as qualitatively verified by the authors. The parameters defining the process noise variance in (7), chosen on the basis of a trial and error procedure, are: $\sigma_1 = 5 \cdot 10^{-3}$, $\sigma_2 = 10^2$ and $\sigma_3 = 10^{-4}$. The standard deviation of the measurement noise is taken equal to $\sigma_\eta = 10^{-1}$. Note only that the factor σ_2 is taken large enough to have a process variance that decreases quite slowly with respect to the degradation times, so as to avoid a

too large reduction of the parameter space spanned by the particles at later times.

In practical applications, Li-ion batteries are usually assumed to be failed when their capacity drops below 80% of its initial value. However, in the case studies shown in this work, the failure threshold will be suitably set in order to both maximize the number of available capacity observations to be processed by the algorithm and enhance the readability of the results, with no loss of generality.

First, we test the algorithm in an ideal situation, i.e., for predicting the RUL of NASA 2 after the initialization of the MLPs of all the particles is performed using the same NASA 2 dataset. Indeed, in this case we expect the best algorithm performance, since the MLP parameters already start from good, optimized values. The failure threshold is here set to a value that is 2% larger than the lowest capacity observation available in the dataset. Figure 3 shows that, after an initial, rather short, adaptation period, the actual RUL (dashed line) is always between the 5th and 95th percentiles of the estimated RUL posterior distribution (green). The initial deviation from the actual RUL, which was not expected since all the MLP particles are trained on the same NASA 2 degradation trajectory, is actually due to the fact that, according to the procedure described in Section 2, the training dataset is normalized in the number of cycles with respect to a cycle horizon that is 50% larger than the true one: hence, the first predictions tend to be approximately 1.5 times larger than the actual RUL (~160 cycles).

Then, we apply the algorithm to the prediction of the RUL of NASA 1 (1850mAh initial capacity). Figure 4 shows that the prognostic performances are satisfactory, although the actual RUL is systematically slightly underestimated. This is motivated by the fact that the degradation curve of NASA 1 (as also those of the other types of battery considered in this work, see Figure 2) shows several positive spikes due to the performances recovery phenomenon (Eddahech, Briat, & Vinassa, 2013). This behavior is actually beneficial to the SOL of the battery, thus leading, in general, to larger RULs. However, these “anomalies” cannot be predicted by the algorithm, which, nevertheless, is shown to be capable of adapting to the changed degradation dynamics and, consequently, to quickly update the RUL posterior pdf estimate.

The batteries used in the previous tests show rather similar trends, even if belonging to different types (NASA 1 1850mAh, NASA 2 2000mAh). So, according to what illustrated in Section 2 with regards to the pre-training procedure, we expect satisfactory results. However, as anticipated in the Introduction, the aim of this work is that of developing a flexible computational prognostic tool capable of automatically dealing with different types of Li-Ion batteries. In order to demonstrate this capability, we now present the prognostic performances of the algorithm when predicting the RUL of a very different type of battery, i.e. the

1100mAh battery (CALCE) taken from the CALCE database (Pecht, 2017). The comparison of the training dataset (NASA 2 from the NASA Ames database) and that used for testing the algorithm (CALCE from the CALCE database) in Figure 5 shows how the two datasets differ both in terms of absolute capacities and lifetimes. In this case, the failure threshold is set to a value that is 20% less of the initial maximum battery capacity. Thus, the pre-training dataset normalization procedure illustrated in Section 2.2 plays an important role for guaranteeing a fast adaptation of the algorithm to the new degradation dynamics. In spite of the fluctuating appearance of the RUL estimate, Figure 6 shows that the RUL predictions are still quite satisfactory and that the MLP-PF behaves as expected. In fact, at earlier times, the capacity observations are still rather close to those of the normalized ones used for the initial MLPs training, so that all the particles (i.e., the MLP networks parameters) do not significantly differ from the training ones, and the corresponding predictions are coherent with the normalized training RUL trajectory (blue, dashed line). As soon as the algorithm starts perceiving the different behavior of the actual observations, at approximately 100 cycles, it suddenly changes the RUL prediction, which accordingly becomes much higher. The weird behavior of the 5th percentile (green line) is due to the presence of the “trivial” particles (see Section 2.2), which tend to adapt more slowly to the new degradation dynamics, thus also being responsible for the initial overestimation of the RUL after approximately cycle 100.

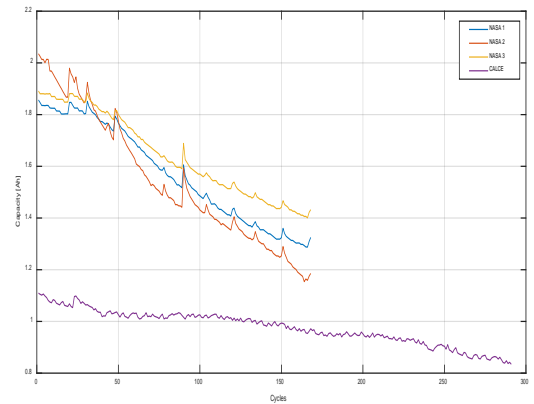


Figure 2: Prognostic Center of Excellence at NASA Ames Research Center [11] and CALCE [12] Battery Group SOL datasets

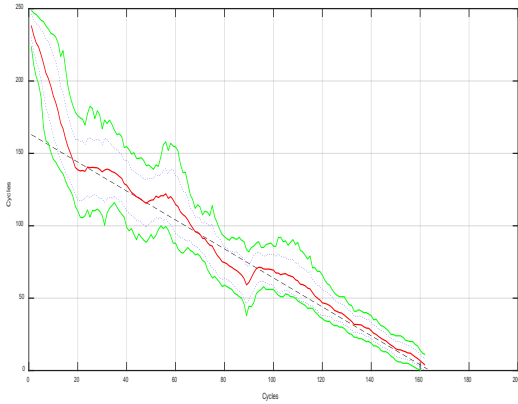


Figure 3: Estimate of the RUL of NASA 2: mean (red), ± 1 standard deviation (grey dotted) and 5th and 95th percentiles (green) of the RUL posterior distribution. The true RUL is the grey, dashed line.

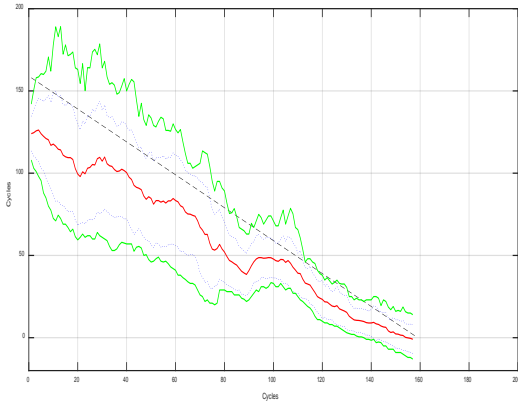


Figure 4: Estimate of the RUL of NASA 1: mean (red), ± 1 standard deviation (grey dotted) and 5th and 95th percentiles (green) of the RUL posterior distribution. The true RUL is the grey, dashed line

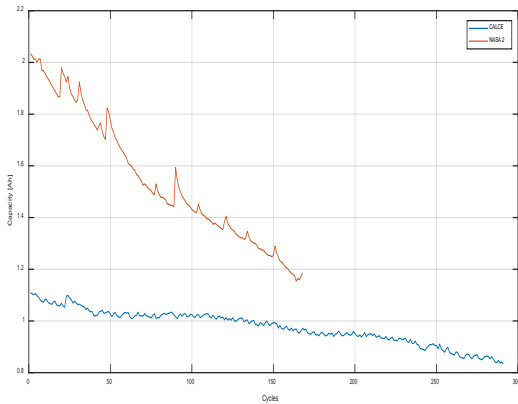


Figure 5: Comparison of the training dataset (NASA 2 from the NASA Ames database, red) and that used for testing the algorithm (CALCE from the CALCE database, blue).

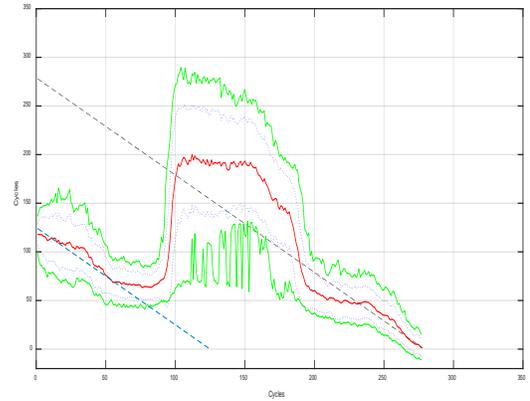


Figure 6: Estimate of the RUL of CALCE: mean (red), ± 1 standard deviation (grey dotted) and 5th and 95th percentiles (green) of the RUL posterior distribution. The true RUL is the grey, dashed line, whereas the blue, dashed line represents the RUL of the normalized NASA 2 dataset used for the pre-training procedure.

4. CONCLUSIONS

In this work we have proposed an original adaptation of an algorithm introduced by some of the same authors for performing adaptive and on-line prognosis of the EOL of Li-Ion batteries. The methodology employs the battery capacity observations, as they become available, within a particle filter framework for adaptively estimating the parameters of the MLP neural network used to represent the relationship between the number of charge-discharge cycles and the battery capacity (i.e., the measurement equation). The particle filter framework then naturally offers the possibility to properly combine the projections into the future of the multiple degradation evolutions given by the MLPs associated to the filter's particles in order to obtain an estimate of the RUL posterior distribution.

The use of generic surrogate models, as the MLP neural networks of this work, for approximating the observation equation significantly increases the adaptability of the prognostic tool with respect to physics-based models. As demonstrated in this work, the advantage of this feature is twofold. First, the algorithm can be effectively applied to many different types of batteries, with very different degradation behaviors, with no need to derive *ad hoc* physics-based models for any possible application; this capability is even further enhanced by the proposed MLP-PF initialization procedure, based on the use of a properly normalized pre-training dataset for restricting the MLP parameters identification space, thus increasing the speed of convergence of the algorithm. Second, the algorithm is capable of re-

configuring itself in case a change of the degradation dynamics occurs, thus still guaranteeing the effectiveness of the prognostic tasks. Note that this last property allows the filter to converge even if no pre-training sets are available, provided the degradation process is not too fast, since the adaptation phase generally requires longer times.

A possible disadvantage related to the use of adaptive surrogate models lies, on the other hand, in the times required for the convergence of the algorithm, which, on average, tend to be larger than those required by similar methods relying on the use of physics-based models. Indeed, a choice must be made between the two types of approaches, mainly depending on the objectives of the application under analysis and the quantity of information available (observations, models, etc.).

Future work on this topic will mainly involve the analysis and the improvement of the algorithm, in order to be able to cope with more realistic operating conditions, for example requiring varying discharge current profiles, possibly also with reference to different degrading power sources systems. Another important future activity is a systematic analysis of the relative importance of the different algorithm parameters (often qualitatively identified in this work on the basis of trial and error procedures) in affecting the algorithm performances. Indeed, this would require to resort also to properly defined prognostic performance measures. On the basis of the available scientific literature and our experience, most probably the process and measurement noise parameters would turn out to be critical for a satisfactory RUL estimation.

REFERENCES

- Arulampalam, M. S., Maskell, S., Gordon, N., & Clapp, T. (2007). A tutorial on particle filters for online nonlinear/nongaussian bayesian tracking. *Bayesian Bounds for Parameter Estimation and Nonlinear Filtering/Tracking*, 50(2), 723–737. <https://doi.org/10.1109/9780470544198.ch73>
- Berecibar, M., Gandiaga, I., Villarreal, I., Omar, N., Van Mierlo, J., & Van Den Bossche, P. (2016). Critical review of state of health estimation methods of Li-ion batteries for real applications. *Renewable and Sustainable Energy Reviews*, 56, 572–587. <https://doi.org/10.1016/j.rser.2015.11.042>
- Bishop, C. M. (1995). Neural networks for pattern recognition. *Journal of the American Statistical Association*, 92, 482. <https://doi.org/10.2307/2965437>
- Cadini, F., Zio, E., & Avram, D. (2009). Monte Carlo-based filtering for fatigue crack growth estimation. *Probabilistic Engineering Mechanics*, 24(3), 367–373. <https://doi.org/10.1016/j.probengmech.2008.10.002>
- Charkhgard, M., & Farrokhi, M. (2010). State-of-charge estimation for lithium-ion batteries using neural networks and EKF. *IEEE Transactions on Industrial Electronics*, 57(12), 4178–4187. <https://doi.org/10.1109/TIE.2010.2043035>
- Darogheh, N., Baniamerian, A., Meskin, N., & Khorasani, K. (2015). A hybrid prognosis and health monitoring strategy by integrating particle filters and neural networks for gas turbine engines. *2015 IEEE Conference on Prognostics and Health Management: Enhancing Safety, Efficiency, Availability, and Effectiveness of Systems Through PHAf Technology and Application, PHM 2015*. <https://doi.org/10.1109/ICPHM.2015.7245020>
- de Freitas, J. F., Niranjan, M., Gee, A. H., & Doucet, A. (2000). Sequential Monte Carlo methods to train neural network models. *Neural Computation*, 12(4), 955–993. Retrieved from <http://www.mitpressjournals.org/doi/abs/10.1162/089976600300015664>
- Doucet, A., Godsill, S., & Andrieu, C. (2000). On sequential Monte Carlo sampling methods for Bayesian filtering. *Statistics and Computing*, 197–208. <https://doi.org/10.1023/A:1008935410038>
- Eddahech, A., Briat, O., & Vinassa, J.-M. (2013). Lithium-ion battery performance improvement based on capacity recovery exploitation. *Electrochimica Acta*, 114, 750–757. <https://doi.org/10.1016/j.electacta.2013.10.101>
- Gordon, N. J., Salmond, D. J., & Smith, A. F. M. (1993). Novel approach to nonlinear/non-Gaussian Bayesian state estimation. *IEE Proceedings F Radar and Signal Processing*, 140(2), 107. <https://doi.org/10.1049/ip-f-2.1993.0015>
- Guo, J., Li, Z., & Pecht, M. (2015). A Bayesian approach for Li-Ion battery capacity fade modeling and cycles to failure prognostics. *Journal of Power Sources*, 281, 173–184. <https://doi.org/10.1016/j.jpowsour.2015.01.164>
- He, W., Williard, N., Osterman, M., & Pecht, M. (2011). Prognostics of lithium-ion batteries based on Dempster-Shafer theory and the Bayesian Monte Carlo method. *Journal of Power Sources*, 196(23), 10314–10321. <https://doi.org/10.1016/j.jpowsour.2011.08.040>
- K.Goebel, B. Saha, P. C. (2008). Prognostics in Battery Health Management. *IEEE Instrumentation & Measurement Magazine*, 33–40. <https://doi.org/10.1002/9781119994053>
- Pecht, M. (2017). Battery Data Set. CALCE. Retrieved from <https://web.calce.umd.edu/batteries/index.html>
- Pinson, M. B., & Bazant, M. Z. (2012). Theory of SEI Formation in Rechargeable Batteries: Capacity Fade, Accelerated Aging and Lifetime Prediction. *Journal of the Electrochemical Society*, 160(2), A243–A250. <https://doi.org/10.1149/2.044302jes>
- Saha, B., & Goebel, K. (2007). Battery Data Set. NASA Ames Prognostics Data Repository. Retrieved from <https://ti.arc.nasa.gov/tech/dash/pcoe/prognostic-data-repository/#battery>

- Sbarufatti, C., Corbetta, M., Giglio, M., & Cadini, F. (2017). Adaptive prognosis of lithium-ion batteries based on the combination of particle filters and radial basis function neural networks. *Journal of Power Sources*, 344(April 2000), 128–140. <https://doi.org/10.1016/j.jpowsour.2017.01.105>
- Schwunk, S., Armbruster, N., Straub, S., Kehl, J., & Vetter, M. (2013). Particle filter for state of charge and state of health estimation for lithium-iron phosphate batteries. *Journal of Power Sources*, 239, 705–710. <https://doi.org/10.1016/j.jpowsour.2012.10.058>
- Vetter, J., Novák, P., Wagner, M. R., Veit, C., Möller, K. C., Besenhard, J. O., ... Hammouche, A. (2005). Ageing mechanisms in lithium-ion batteries. *Journal of Power Sources*, 147(1–2), 269–281. <https://doi.org/10.1016/j.jpowsour.2005.01.006>
- Wang, D., Yang, F., Zhao, Y., & Tsui, K.-L. (2017). Battery remaining useful life prediction at different discharge rates. *Microelectronics Reliability*, 78, 212–219. <https://doi.org/10.1016/j.microrel.2017.09.009>
- Wu, L., Fu, X., & Guan, Y. (2016). Review of the Remaining Useful Life Prognostics of Vehicle Lithium-Ion Batteries Using Data-Driven Methodologies. *Applied Sciences*, 6(6), 166. <https://doi.org/10.3390/app6060166>
- Francesco Cancelliere** obtained the Bachelor in Energy Engineering in 2016 at Politecnico di Milano, where he is going to succeed in the Master of Science in Energy Engineering, specialising in “Power Production”. His current work of master thesis is focused on Battery Health Monitoring, aimed at the diagnosis and residual life prognosis of Li-ion batteries and Fuel Cells, in a probabilistic framework. The methodologies of interest are based on particle filter strategies, combined with models generated by artificial neural networks.
- Marco Giglio** is Full Professor of Mechanical Design and Strength of Materials, and works in the Department of Mechanical Engineering at Politecnico di Milano, Italy. His research fields are novel methods for SHM application, ballistic damage and evaluation of the residual strength, methods of fatigue strength assessment in mechanical components subjects to multiaxial state of stress, design and analysis of helicopter components with defects, optimization of structures for energy application. He is the author of over 150 scientific papers in international journals and conferences and is a member of scientific associations (AIAS, Italian Association for the Stress Analysis, IGF, Italian Group Fracture).

BIOGRAPHIES

Francesco Cadini is assistant professor at the Department of Mechanical Engineering of the Politecnico di Milano. His main research efforts are currently devoted to the quantitative treatment of uncertainties affecting the models for risk assessment and mitigation in modern engineering systems. In particular, his activities are mainly focused on the development and application of i) sequential Monte Carlo algorithms (particle filters) for state estimation and prediction with applications to system diagnostic and prognostic, ii) variance reduction methods for more efficient Monte Carlo-based uncertainty analysis, iii) surrogate modeling (neural networks, polynomial chaos expansion, kriging, fuzzy logic, support vector machine, etc.) for model identification, time series prediction and optimal control in complex engineering systems.

Claudio Sbarufatti is a research scientist and Assistant Professor with the Department of Mechanical Engineering at Politecnico di Milano, Italy. His research interests include model-based diagnosis and prognosis of mechanical and aerospace components, Monte-Carlo methods for Bayesian model updating and filtering, inverse problems for load monitoring, distributed sensing, system failure modeling, impact modeling on composite structures. He is currently involved in the management of international projects mainly focused on structural health monitoring, load monitoring and residual life prognosis.